Electronic Supplementary Material (ESI) for Nanoscale.

Electronic Supplementary Information (ESI)

Surface effects on a photochromic spin-crossover iron(II) molecular switch adsorbed on highly oriented pyrolytic graphite.

Lorenzo Poggini,* Giacomo Londi, Magdalena Milek, Ahmad Naim, Valeria Lanzilotto, Brunetto Cortigiani, Federica Bondino, Elena Magnano, Edwige Otero, Philippe Sainctavit, Marie-Anne Arrio, Amélie Juhin, Mathieu Marchivie, Marat M. Khusniyarov, Federico Totti,* Patrick Rosa, Matteo Mannini.

Table S1. Atomic concentration estimated by XPS for SCO sub-monolayer (0.7ML) evaporated on HOPG

Element	**Fe*2p***	**N*1s***	**B*1s***	**S*2p***
Experimental	5.2	65.8	13.1	15.9
Theoretical	6.7	66.7	13.3	13.3

Table S2**.** Binding Energies (B.E.) of the spectral components obtained for the Fe*2p* XPS by a least square fitting procedure. The integrated areas are reported like percentages of each component.

Components	**A+A'**	**B+B'**	**C+C'**	**D+D'**	**E+E'**
	%; B.E.	%; B.E.	%; B.E.	%; B.E.	%; B.E.
158K	33.3%; 708.9 eV	25.1%; 709.9 eV	17.9%; 712.1 eV	13%; 715.6 eV	10.7%; 718.4 eV
192K	22.1%; 708.9 eV	35.3%; 710.0 eV	17.9%; 712.0 eV	15.1%; 715.3 eV	9.6%; 718.3 eV
245K	9.2%; 708.8 eV	37.0%; 709.9 eV	23.9%; 712.0 eV	18.3%; 715.3 eV	11.6%; 718.3 eV
297K	5.9%; 708.9 eV	32.4%; 710.0 eV	31.4%; 712.0 eV	18.6%; 715.6 eV	11.4%; 718.4 eV
297K + λ282nm	5.7%; 708.9 eV	34.9%; 710.0 eV	29.2%; 711.9 eV	18.5%; 715.5 eV	11.7% 718.2 eV

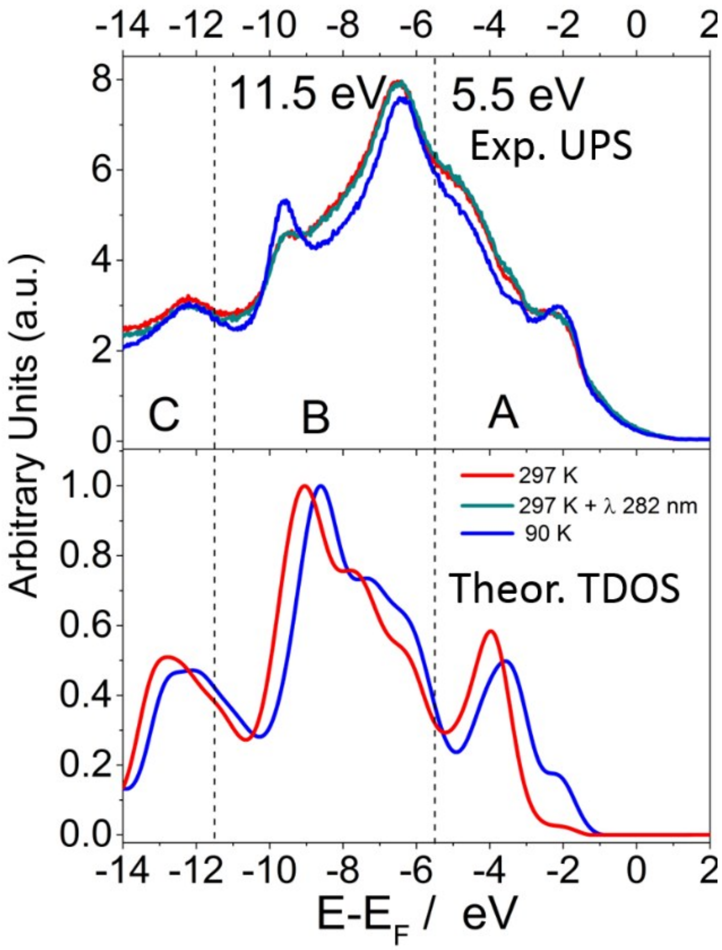

Figure S1. Computed DOS for the 1-par-HS (red line) and 1-par-LS (blue line), where A, B, and C indicate the three characteristic energy regions of the **1** system. **EXP:** UPS spectra from -14 eV to 0 eV ($E-E_F$) at 297K (red line), 90K (blue line) and after UV irradiation at 297K (green line). The two vertical lines delimit the valence-Fermi region (A region), from the semi-core (B) region, from the core (c) region on the spectra.

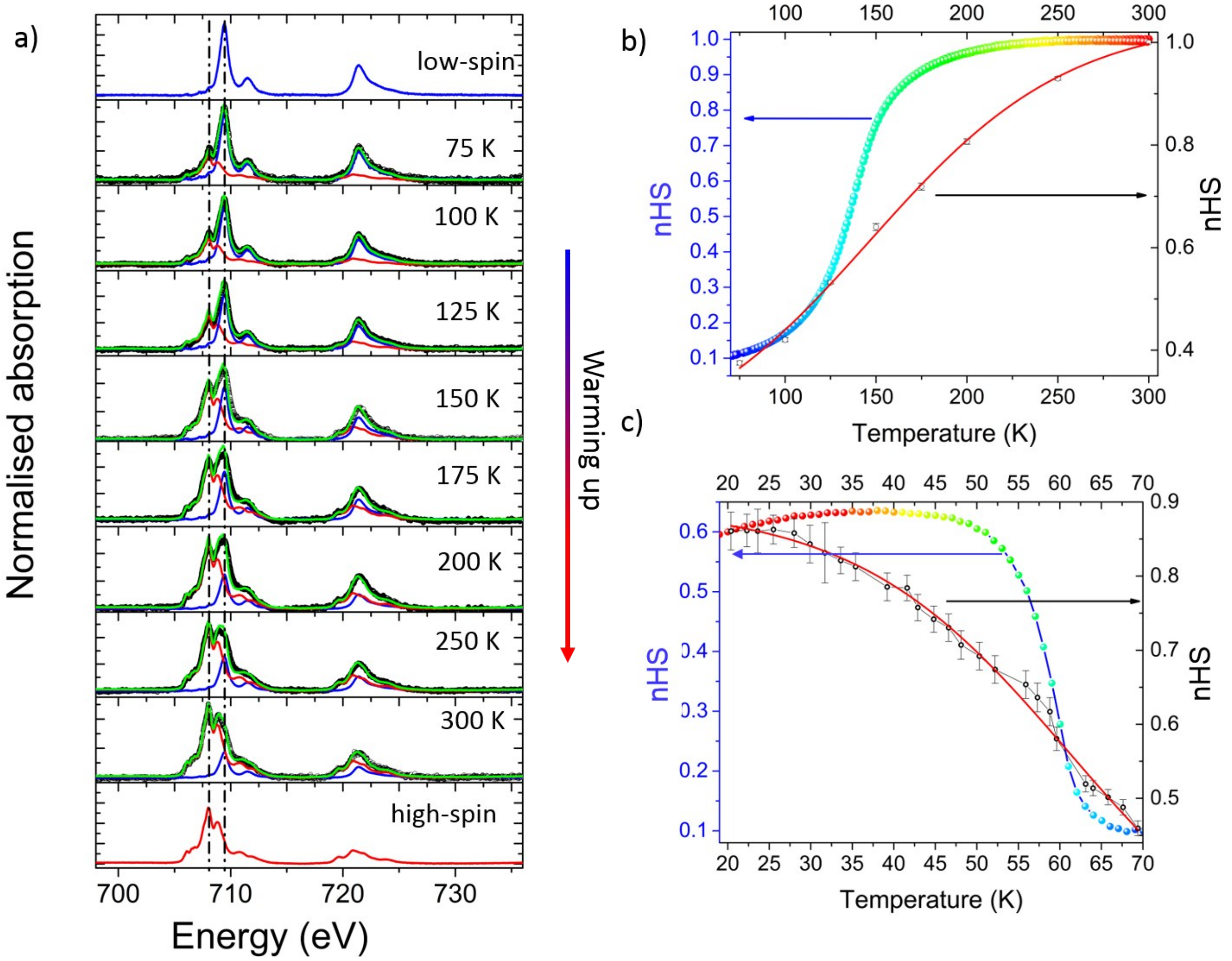

Figure S2. (a) Temperature evolution of the Fe$L_{2,3}$ edges XAS spectra for a sub monolayer deposit of **1** on HOPG (empty circles), along with best fitting lines (green line), calculated as described in the Methods section. High-spin Fe(II) and low-spin Fe(II) contributions are blue and red lines, respectively. The spectra, taken on the same spot of the sample, point out the occurrence of a reversible thermally driven high-spin Fe(II) to low-spin Fe(II) conversion on lowering the temperature, in line with an entropy driven SCO process at the sub-monolayer level. Broken vertical lines correlate spectral features belonging to the different spin states throughout the series. (b and c) high-spin Fe (II) thermal distribution profile (empty circles) obtained from XAS spectra taken before (b) and after (c) laser light irradiation at 4 K for a 4 nm deposit of **1** on freshly cleaved HOPG. In b) and c) the red line is the fit of empty black dots by a Boltzman distribution, giving a $T_{1/2}$ of 146 ± 8K and 61 ± 5K respectively. Data measured for the bulk sample are taken from ref. S1 and are reported as wide coloured bands for comparison.

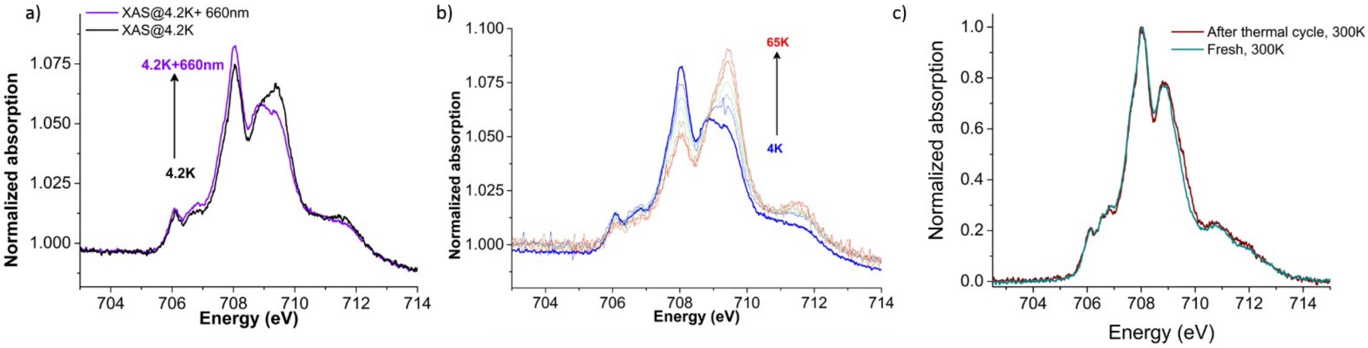

Figure S3. XAS spectra of 0.7ML deposit of **1** on HOPG at 4.2K: a) before and after irradiation at 660nm - LIESST effect, b) upon subsequent warming - thermal relaxation, c) comparison of the XAS spectra before and after a thermal cycle (300K -4K - 300K).

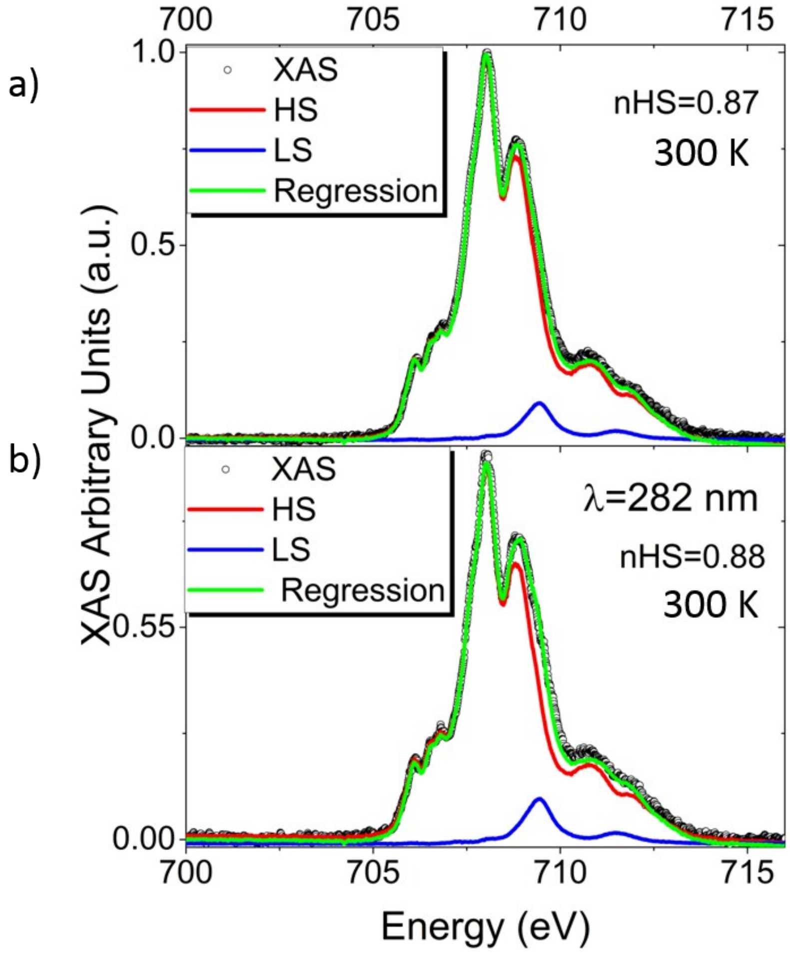

Figure S4. XAS spectrum of 0.7ML deposit of **1** on HOPG, before a) and after UV exposure b).

Table S3: Calculated bond lengths and angles involving the iron metallic core in comparison with experimental data, obtained in ref. [s1], alongside computed θ values, defined as the angle between the plane determined by the phenanthroline plane and the thiophene plane. Mean absolute deviation are also reported, where $MAD = \frac{1}{n}\sum_{i}^{n}\left|x_{cal} - x_{exp}\right|$. See Fig. S4 for the labelling.

	1-LS [s1]	**1**-LS-anti	**1**-LS-par	**1**-HS [s1]	**1**-HS-anti	**1**-HS-par
	Bond length (Å)			*Bond length (Å)*		
Fe-N1	1.967	1.972	1.980	2.184	2.224	2.207
Fe-N2	1.969	1.963	1.967	2.179	2.218	2.216
Fe-N6	1.999	1.989	1.993	2.144	2.138	2.139
Fe-N3	2.002	2.002	2.003	2.164	2.169	2.152
Fe-N7	2.005	1.989	1.982	2.142	2.130	2.133
Fe-N4	2.008	2.003	2.010	2.173	2.161	2.200
MAD	-	0.01	0.01	-	0.02	0.02
	Angle (degrees)			*Angle (degrees)*		
N2-Fe-N6	176.14	177.84	176.56	169.26	166.48	167.78
N1-Fe-N7	177.29	177.90	176.24	171.59	174.35	172.60
N3-Fe-N4	178.74	179.13	178.89	177.91	176.82	179.08
MAD	-	0.90	0.54	-	2.21	1.22
$\theta_{anti(1,2)}$	61.8/72.6	61.1/72.5	-	65.2/74.5	65.3/67.7	-
$\theta_{par(1,2)}$	64.4/72.6	-	51.6/77.0	66.9/74.5	-	52.2/75.1

S1 M. Milek, F. F. W. Heinemann and M. M. M. Khusniyarov, *Inorg. Chem.*, 2013, **52**, 11585–92.